ISBN: 978-3-95450-208-0 doi:10.18429/JACoW-IPAC2019-WEPGW004

WIRE SCANNER FOR HIGH INTENSITY ION BEAM*

A. Beller†, D. Bondoux, F. Bouly, LPSC, Université Grenoble-Alpes, CNRS/IN2P3, Grenoble, France

Abstract

The goal of the project is to develop a Wire-Scanner compatible with low energy - high intensity ion beams and adaptable to various beam chamber diameters. The purpose is to obtain the 2D beam profile by passing measurement wires through the beam. Thanks to a high speed passage of measurement wires, it allows to avoid "disrupting" the beam passage, and can be considered as a non-destructive diagnosis. Wires heating and measuring issues have been solved by using tungsten wires kept in tension by a mechanical system. All driving and signal measurements are performed by a PXI based system. The synchronization of the measurements is guaranteed by an analog input board recovering the wires current and the translator position, the latter being carried out by a laser sensor. Besides this technological aspect, an optimization algorithm for beam profile reconstruction from measured data under Gaussian hypothesis has been developed. The standalone system and first experimental results are presented.

INTRODUCTION

During the commissioning and exploitation of a particle accelerator, beam diagnostics are used to qualify the accelerated particles beam properties. The used diagnostics are most often destructive. However, a non-destructive measurement tool would be of great benefits for the MYRRHA (Multi-purpose hYbrid Research Reactor for High-tech Applications) linac [1] operation and commissioning (especially for the injector). It would allow periodic monitoring of the beam profile with minimized beam perturbations. The envisaged solution is a wire-scanner that is an almost non-destructive diagnosis [2]. This apparatus consists of a Pfeiffer Vacuum motorized translator with ball screw driving a fork with three conductor wires of small diameters. This appliance goes down into the vacuum chamber and then returns to its initial position. The control system of the Mitsubishi motor (HG-JR1034B) is ensured by National Instrument environment composed of a frame (PXIe-1071) and a motion controller (PXI-7340) with its motion interface (UMI-7772). Thanks to the linear translation see Fig. 1), the particle beam hits the wires during their passage and thus this interaction creates a current in each wire. A LabVIEW program displays a graph of the measured current versus the translator position for each wire. The measurements synchronization (translator position and three measured currents) is ensured by an acquisition board PXIe-4464, owing 4 analog inputs. The laser sensor OptoNCDT 1420 enables to feedback the translator position with a very good accuracy. The maximum sampling rate is 4 kHz (limited by the laser sensor). By mathematical reconstruction, the profile of the beam within the vacuum chamber at the wire-scanner position is evaluated.

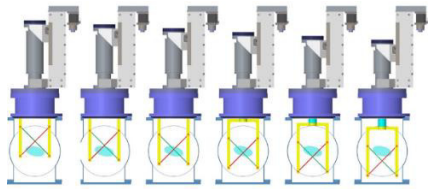

Figure 1: Displacement of measurement wires though the beam.

This wire-scanner was designed for a continuous beam in MYRRHA LEBT (Low Energy Beam Transport) [3], see Table 1.

Table 1: Continuous Beam Characteristics of MYRRHA LEBT

Characteristic	Values
Energy E	30 keV
Intensity I	3.5-10 mA
RMS transverse beam size σ	10-20 mm

The "worst case" of LEBT beam is E=30 keV; I=10 mA; $\sigma_x = \sigma_y = 10$ mm.

CHOICE OF WIRE'S MATERIAL

The choice depends of the admissible temperature limit and of the current recovery performance when the wires pass through the beam. Generally, the measuring wires are carbon or tungsten wires. For the simulations, the diameter for carbon is 33 µm and 80 µm for tungsten.

Estimated Current

About the current recovery, the measurement is based on SEY (Secondary Emission Yield) evaluation given by [4]:

$$SEY = 0.01 \cdot L_s \frac{dE}{dx}\bigg|el \left[1 + \frac{1}{1 + (5.4 \cdot 10^{-6}\, E/A_p)}\right] \quad (1)$$

$$L_s = (3.68 \cdot 10^{-17} N Z^{1/3})^{-1} \quad (2)$$

Where $\frac{dE}{dx}|el$ is electronic energy loss (eV/cm), E is the kinetic energy (eV), A_p is mass of the particle (amu), N is the number of atoms per unit volume (atoms/cm^3) and Z is the atomic number (-). At 30 keV, the estimated SEY evaluation is near 4 for these two materials. It means that: for one proton, which interacts with the wire material, 4 secondary electrons should be emitted. The production of secondary electron is proportional to the number of incident proton. Using SEY evaluation enables to estimate the current and then, to size the preamplifier for the wire current.

* Part of this work had been supported by the European Atomic Energy Community's (EURATOM) H2020 Programme under grant agreement n°662186 (MYRTE project).
† alexis.beller@lpsc.in2p3.fr

ISBN: 978-3-95450-208-0 doi:10.18429/JACoW-IPAC2019-WEPGW004

The expected current, with Gaussian hypothesis, is done by:

$$I_{mes} = SEY \iint_{wire} \frac{I}{2\pi\sigma_x\sigma_y} e^{-\frac{1}{2}\left(\frac{x^2}{\sigma_x^2}+\frac{y^2}{\sigma_y^2}\right)} dxdy \quad (3)$$

Where I is the beam current, σ_x and σ_y are RMS transverse beam sizes. The expected current for the specified beam is shown in Figure 2. The expected current is larger for tungsten than carbon due to the wire diameter. The maximum current obtained should be 130 µA for tungsten.

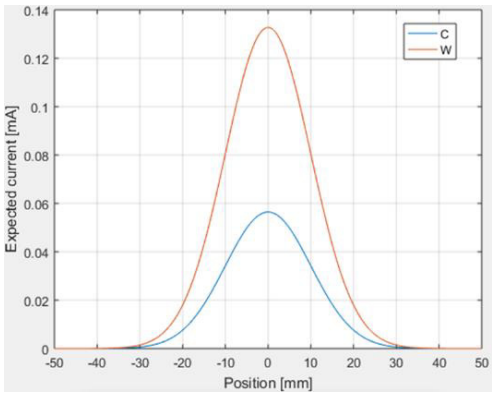

Figure 2: Expected current for the carbon (blue) and tungsten (orange) wire in function of the wire position.

Thermionic Emission

The thermionic emission is a process that perturbs the signal from secondary emission. It depends on the temperature of the wire. Some supplementary electrons are emitted and the reading of the useful current for the profile pattern will be skewed. This effect can be estimated as [5]:

$$J = A \cdot T^2 \cdot e^{-\frac{\phi(T)}{kT}} \quad (4)$$

Where A is the Richardson-Dushman constant, T is the temperature (K), $\Phi(T)$ is the work function of material (equivalent for carbon and tungsten: ≈4-5 eV) and k is the Boltzmann constant. Up to 2000 K, the thermionic emission can be neglected. It is preferable that the wire temperature does not exceed this threshold. For example, Table 2 shows the error measurements, for a tungsten wire, for the considered beam.

Table 2: Effect of the Thermionic Emission on the Measurements

Reached temperature by wires [K]	Current induced by thermionic effect [µA]	Measurements relative error [%]
2047	2	1.54
2322	55	42.3
2577	500	384

Estimated Temperature

The thermal load on wire induced by the beam could, in the worst case, damage and break the wire. At 30 keV, all the energy particles remains in the wire. The temperature elevation due to the beam can be calculated as [6]:

$$\Delta T = \frac{N_{part}(x,y) \cdot \Delta E}{\rho \cdot Cp(T) \cdot V_f} \quad (5)$$

Where N_{part} is number of particles following the position on the transverse axis of accelerator reference (-), ΔE is the energy deposited in the wire per particle (J), ρ is material density, Cp(T) is the specific heat capacity of the material of the wire, and V_f is the volume of the wire.

In approximation, the wire cooling is dominated by radiation, described by Stefan-Boltzmann law, and the conductive cooling is neglected. The temperature losses is:

$$\frac{dT}{dt} = \frac{\varepsilon \cdot \sigma_B \cdot A_f \left(T^4 - T_{amb}^4\right)}{\rho \cdot Cp(T) \cdot V_f} \quad (6)$$

Where ε the emissivity of the wire material (-), σ_B is the Stefan-Boltzmann constant, A_f the area of the body (m²), T its temperature (K) and T_{amb} the ambient temperature (298 K generally). The thermal model of this system is the combination of the last two equations (5 and 6). After a succession of round-trip at a velocity of 0.2 m/s, the wire do not exceed the thermionic emission threshold (see Fig. 3). With a good choice of velocity and appropriate withdrawal period between each passage into the beam, the tungsten wire is suitable for this application in term of expected current and temperature.

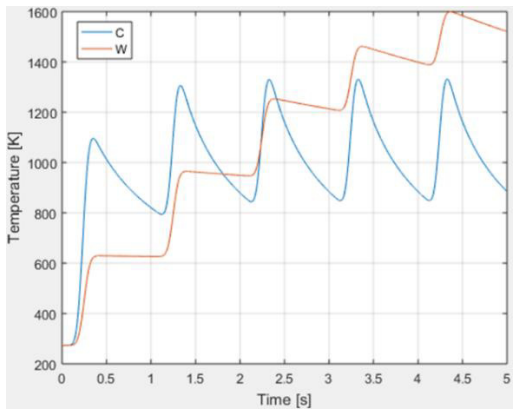

Figure 3: Evolution of the temperature in the middle of the wire over the time for the carbon (blue) and the tungsten (orange) for a succession of round-trip. Velocity=0.2 m/s; Waiting time out of beam=1 s.

EXPERIMENTAL RESULTS

Test Bench

The wire-scanner was, installed on a test bench at Laboratoire de Physique Subatomique et Cosmologie (LPSC), see Fig. 4, to validate its control and operation principle. The tests bench consists of a duoplasmatron source that produces deuterium d^+ beam with a maximum energy of 30 keV and a maximum current of 1 mA (continuous beam). A magnetic quadrupole, with integrated steerer, enables to focus/defocus the beam and corrects its trajectory. The wire-scanner is placed vertically relative to

ISBN: 978-3-95450-208-0 doi:10.18429/JACoW-IPAC2019-WEPGW004

the beam line. After the wire scanner, a dipole deviates the beam to a beam dump.

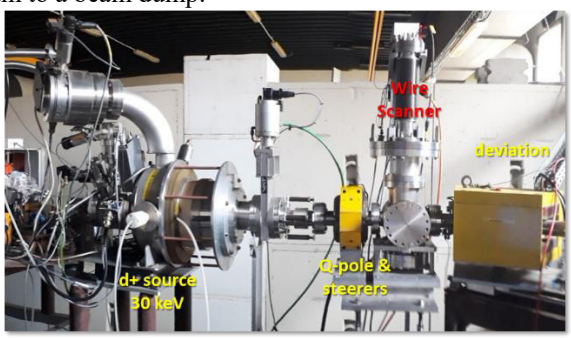

Figure 4: Test bench at LPSC.

Reconstruction of 2D Beam Profile

Several measurements were carried out. From the three voltage-translator position set of data (obtained thanks to LabVIEW program), measurements are processed thanks to a self-standing application developed as a MATLAB application. It allows to identify some information related to the beam such as the position of beam center, the RMS transverse size σ_x and σ_y. The "Identification" method is the result of the minimization of an error function by taking into account the set of measurement wires. The error function corresponds to the area delimited between the measured values and the simulated values (assuming a bi-Gaussian beam) versus translator position. The Figure 5 shows an example of beam profile obtained on this test bench.

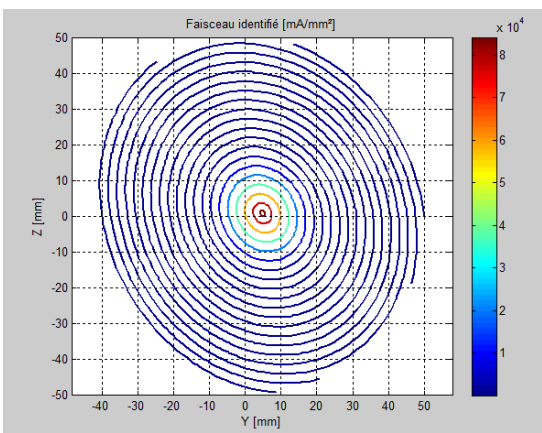

Figure 5: 2D profile of the beam for a current of 250 µA, focusing of 12 keV and 0 A in quadrupole.

Test Line Tuning Effects on the Beam Profile

By changing the extraction tunings of the source and the quadrupole focusing strength, we have succeeded to highlight the influence these different parameters on the beam profile. For example, the Figure 6 points out the effect of the quadrupole, placed just before the wire-scanner (see Figure 4). On x-axis (horizontal axis), the beam is defocused when the quadrupole current rises. On y-axis (vertical axis), the beam is focused and the rms size reached a minimum (3.1 mm) for 4 A in quadrupole. Afterwards, the size on y-axis increases, due to the focusing point that is getting closer and closer to the quadrupole.

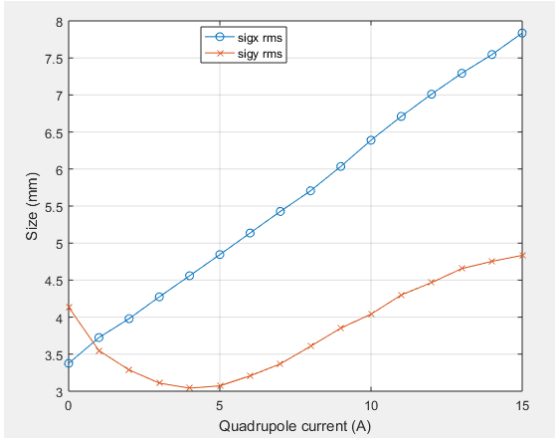

Figure 6: Influence of the quadrupole current on the beam size.

In addition, the source focusing voltage parameter has a huge impact on the beam profile (see Fig. 7). On the left, the focusing voltage is 12 kV and assuming a bi-Gaussian beam is correct. Adversely, for a focusing voltage of 11 kV (right plot), it is impossible to reconstruct the beam profile and the Gaussian approximation cannot be used.

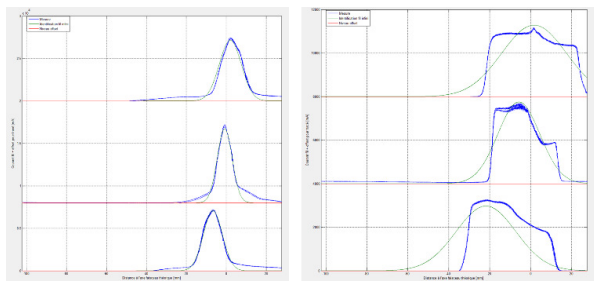

Figure 7: Influence of the source focusing voltage on measured current plot (12 kV on the left and 11 kV on the right).

CONCLUSION

Using some diagnoses is crucial for the exploitation of beam lines. They provide information about the beam and help to optimize the beam transport. Many diagnostics are destructive and cannot be used without perturbing the accelerator operation. The wire-scanner is almost a non-destructive apparatus and its main advantage is that it can be used for on-line tuning of an injector. It has been constructed taking into account the effect of the vacuum such as the wire heating, the secondary electron emission. An electronic board has been designed in function of the expected beam in the MYRRHA LEBT. This device has been tested on a test bench and it operates successfully for low intensity ion beam. The approximation by assuming a bi-Gaussian beam seems correct in most of the cases. The huge advantage of this diagnosis is the measurements speed to draw the 2D profile and it is very interesting to use it for the commissioning and tuning of a linac. The next step will be to test the device on the MYRRHA LEBT (now located in Louvain-la-Neuve, Belgium) with higher current amplitude (~10 mA).

ISBN: 978-3-95450-208-0 doi:10.18429/JACoW-IPAC2019-WEPGW004

REFERENCES

[1] D. Vandeplassche *et al.*, "Integrated Prototyping in View of the 100 MeV Linac for Myrrha Phase 1", in *Proc. 9th Int. Particle Accelerator Conf. (IPAC'18)*, Vancouver, Canada, Apr.-May 2018, pp. 661-664. doi:10.18429/JACoW-IPAC2018-TUPAF003

[2] P.Forck, Lecture notes on beam instrumentation and diagnostics, Joint Universities Accelerator School, Archamps, France, Feb 2018.

[3] F. Bouly *et al.*, "Commissioning of the MYRRHA Low Energy Beam Transport Line and Space Charge Compensation Experiments", in *Proc. 8th Int. Particle Accelerator Conf. (IPAC'17)*, Copenhagen, Denmark, May 2017, pp. 1226-1229. doi:10.18429/JACoW-IPAC2017-TUOBA2

[4] D.Kramer, "Design and Implementation of a Detector for High Flux Mixed Radiation Fields", PhD thesis, 2008

[5] B. Cheymol, "Development of beam transverse profile and emittance monitors for the CERN LINAC4", PhD Thesis, 2011.

[6] B. Cheymol, "Effects of Energy Deposition Models and Conductive Cooling on Wire Scanner Thermal Load, Analytical and Finite Element Analysis Approach", in *Proc. 57th ICFA Advanced Beam Dynamics Workshop on High-Intensity and High-Brightness Hadron Beams (HB'16)*, Malmö, Sweden, Jul. 2016, pp. 221-225. doi:10.18429/JACoW-HB2016-MOPL016